

Chapter 10

Neural Network Modeling of Voluntary Single-Joint Movement Organization I. Normal Conditions

Vassilis Cutsuridis

Abstract Motor learning and motor control have been the focus of intense study by researchers from various disciplines. The neural network model approach has been very successful in providing theoretical frameworks on motor learning and motor control by modeling neural and psychophysical data from multiple levels of biological complexity. Two neural network models of voluntary single-joint movement organization under normal conditions are summarized here. The models seek to explain detailed electromyographic data of rapid single-joint arm movement and identify their neural substrates. The models are successful in predicting several characteristics of voluntary movement.

10.1 Introduction

Voluntary movements are goal-directed movements triggered either by internal or external cues. Voluntary movements can be improved with practice as one learns to anticipate and correct for environmental obstacles that perturb the body. Single-joint rapid (ballistic) movements are goal-directed movements performed in a single action, without the need for corrective adjustments during its course. They are characterized by a symmetric bell-shaped velocity curve, where the acceleration (the time from the start to the peak velocity) and deceleration (the time from the peak velocity to the end of movement) times are equal [3]. Similar velocity profiles have also been observed in multi-joint movements [11].

The electromyographic (EMG) pattern of single-joint rapid voluntary movements in normal subjects is also very characteristic. It is characterized by alternating bursts of agonist and antagonist muscles [28]. The first agonist burst provides the impulsive force for the movement, whereas the antagonist activity provides the braking force

Vassilis Cutsuridis
Centre for Memory and Brain, Boston University, Boston, MA, USA
e-mail: vcut@bu.edu

to halt the limb. Sometimes a second agonist burst is needed to bring the limb to the final position [1, 4, 5, 6, 23, 24, 25, 26, 27, 36]. The combination of the agonist–antagonist–agonist bursts is known as the triphasic pattern of muscle activation [28]. An excellent review on the properties of the triphasic pattern of muscle activation and the produced movement under different experimental conditions can be found in Berardelli and colleagues [2].

The origin of the triphasic pattern and whether it is controlled by the nervous system has been long debated [33]. In a review paper by Berardelli and colleagues [2], three conclusions were made: (1) the basal ganglia output plays a role in the scaling of the first agonist burst size, (2) the corticospinal tract has a role in determining spatial and temporal recruitment of motor units, and (3) the proprioceptive feedback is not necessary to the production of the triphasic pattern, but it contributes to the accuracy of both the trajectory and the end point of ballistic movements. That means that the origin of the triphasic pattern of muscle activation *may* be a central one, but afferent inputs can also modulate the voluntary activity.

10.2 Models and Theories of Motor Control

Motor learning and motor control have been the focus of intense study by researchers from various disciplines. The experimental researchers interested in motor learning investigate how practice facilitates skill acquisition and improvement. The theoretical/computational researchers interested in motor control have investigated which movement variables are controlled during movement from the nervous system [33]. Many computational models of motor control have been advanced over the years [14]. These models include the equilibrium point hypothesis [20], dynamical system theory [32], the pulse-step model [22], the impulse-timing model [35], the dual-strategy hypothesis [14], models about minimizing movement variables [34], and neural network models [8, 9, 10, 13, 17, 15, 16, 18].

The neural network model approach has been very successful in providing theoretical frameworks on motor learning and motor control by modeling neural and psychophysical data from multiple levels of biological complexity. In particular, the vector integration to endpoint (VITE) and factorization of muscle length and muscle tension (FLETE) neural network models of Bullock, Grossberg, and colleagues [7, 8, 9, 10, 13] have provided qualitative answers to questions such as how can a limb be rotated to and stabilized at a desired angle? How can movement speed from an initial to a desired final angle be controlled under conditions of low joint stiffness? How can launching and braking forces be generated to compensate from inertial loads? The VITE model was capable of generating single-joint arm movements, whereas the FLETE model afforded independent voluntary control of joint stiffness and joint position, and incorporated second-order dynamics, which played a large role in realistic limb movements. Variants of the FLETE model [9] have been successful in producing realistic transient muscle activations, such as the triphasic pattern of muscle activation observed during rapid, self-terminated movements.

Despite their successes, the VITE and FLETE models have several limitations. First, in an attempt to simulate the joint movement and joint stiffness, Bullock and Grossberg speculated the presence of the two partly independent cortical processes [30], a reciprocal signal of antagonist muscles responsible for the joint rotation, and a co-contraction signal of antagonist muscle responsible for joint stiffness. However, neither the VITE-FLETE model studies [9] nor the Humphrey and Reed [30] experimental study has identified the exact neural correlates (i.e., cell types) for the reciprocal activation and co-contraction of antagonist muscles.

Second, they failed to provide functional roles of experimentally identified neurons in primary motor cortex (area 4) and parietal cortex (area 5), such as the phasic

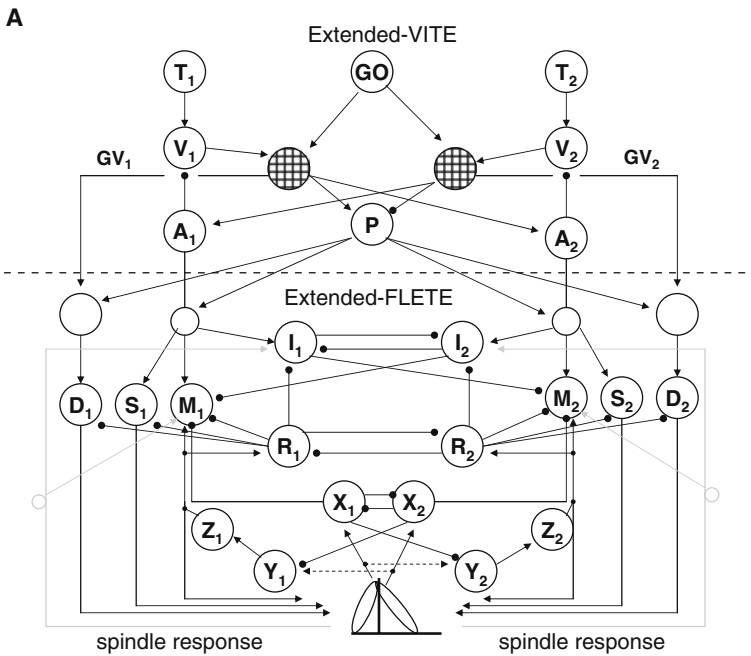


Fig. 10.1: Extended VITE–FLETE models without dopamine (DA). (A and B) *Top*: Extended-VITE model for variable-speed trajectory generation. *Bottom*: Extended-FLETE model of the opponent processing spinomuscular system. *Arrow lines*: excitatory projections; *solid dot lines*: inhibitory projections; *dotted arrow lines*: feedback pathways from sensors embedded in muscles. *GO*: basal ganglia output signal; *P*: bidirectional co-contraction signal; *T*: target position command; *V*: DV activity; *GV*: DVV activity; *A*: current position command; *M*: alpha motoneuronal (MN) activity; *R*: rensaw cell activity; *X, Y, Z*: spinal inhibitory interneuron (IN) activities; *I_a*: spinal type a inhibitory IN activity; *S*: static gamma MN activity; *D*: dynamic gamma MN activity; *I, 2*: antagonist cell pair.

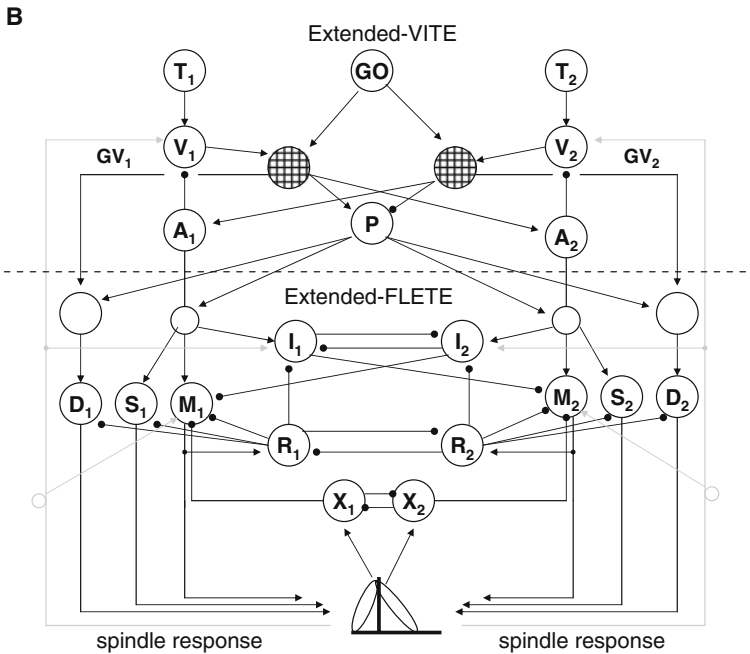


Fig. 10.1: (continued)

cells, the tonic cells, the reciprocal cells, and the bidirectional cells known to play a role in voluntary movement initiation and control [19, 21].

Third, they failed to identify the site of origin of the triphasic pattern of muscle activation [2]. Is the triphasic pattern cortically or subcortically originated [2]? If cortically originated, are the agonist and antagonist bursts generated from experimentally identified cortical cell types? Does the afferent feedback from the muscle spindles to the spinal cord play any role in maintenance of this pattern? Does the feedback from the muscle spindles to the cortex play a role in the generation of the second agonist burst?

These limitations were addressed successfully by the extended VITE–FLETE with dopamine models of Cutsuridis and Perantonis [18] and Cutsuridis [15, 16, 17]. These models have answered issues concerning voluntary movement and proprioception in normal and Parkinsonian conditions. The temporal development of these models in normal conditions (i.e., without dopamine) is reviewed in detail in the next section.

10.3 The Extended VITE–FLETE Models Without Dopamine

Figures 10.1a, b depict the extended VITE–FLETE models without dopamine of voluntary movement and proprioception [15, 16, 17, 18]. Both models were based

on known corticospinal neuroanatomical connectivity. Detailed description and complete mathematical formalism of the models can be found in Cutsuridis and Perantonis [18] and Cutsuridis [15, 17]. Both extended VITE–FLETE without dopamine models, while they preserved the original VITE–FLETE model’s capability of generating rapid single-joint movements and affordance of independent voluntary control of joint stiffness and joint movement, they were extended it in three fundamental ways.

In a behavioral neurophysiology task, Doudet and colleagues [19] trained monkeys to perform fast flexion and extension elbow movements while they recorded from their primary motor cortex. Three classes of movement-related neurons were identified according to their activity during the movement: (1) neurons showing a reciprocal discharge pattern for flexion and extension movements (reciprocal neurons), (2) neurons whose activity changed for only one direction (unidirectional neurons), and (3) neurons whose activity decreased or increased for both directions of movement (bidirectional neurons). In the extended VITE–FLETE with dopamine model of Figure 10.1a [15, 16, 18] functional roles to the cortically identified reciprocal [19], bidirectional [19], phasic MT and tonic neurons were assigned. An arm movement difference vector (DV) was computed in parietal area 5 from a comparison of a target position vector (TPV) with a representation of the current position called perceived position vector (PPV). The DV signal then projected to area 4, where a desired velocity vector (DVV) and a nonspecific co-contractive signal (P) [30] were formed. A voluntarily scalable GO signal multiplied (i.e., gated) the DV input to both the DVV and the P in area 4, and thus volitional sensitive velocity and nonspecific co-contractive commands were generated, which activated the lower spinal centers. The DVV and P signals corresponded to two partly independent neuronal systems with the motor cortex [30].

The output of the basal ganglia (BG) system, which represented the activity of the GPi was modeled by a GO signal:

$$G(t) = G_0(t - \tau_i)^2 u[t - \tau_i] / (\beta + \gamma(t - \tau_i)^2), \quad (10.1)$$

where G_0 amplified the G signal, i was the onset time of the i th volitional command, β and γ are free parameters, and $u[t]$ was a step function that jumped from 0 to 1 to initiate movement. The difference vector (DV), which represented cortical area’s 5 phasic cell activity, was described by

$$\frac{dV_i}{dt} = 30(-V_i + T_i - A_i), \quad (10.2)$$

where T_i was the target position command and A_i was the current limb position command.

In contrast to the original VITE–FLETE model [9, 10], in the extended VITE–FLETE models [15, 16, 17, 18], the desired velocity vector (DVV) represented the activity of cortical area’s 4 phasically activated reciprocal neurons [19], and it was organized for the reciprocal activation of antagonist muscles. It was defined by

$$u_i = [G(V_i - V_j) + B_u]^+, \quad (10.3)$$

where i, j designated opponent neural commands and B_u was the baseline activity of the phasic-MT area 4 cell activity.

The co-contractive vector (P) represented area's 4 phasic activity of bidirectional neurons (i.e., neurons whose activity decreases or increases for both directions of movement [19]), and it was organized for the co-contraction of antagonist muscles (see columns 1 and 3 of Fig. 10.2). It was given by

$$P = [G(V_i - V_j) + B_P]^+. \quad (10.4)$$

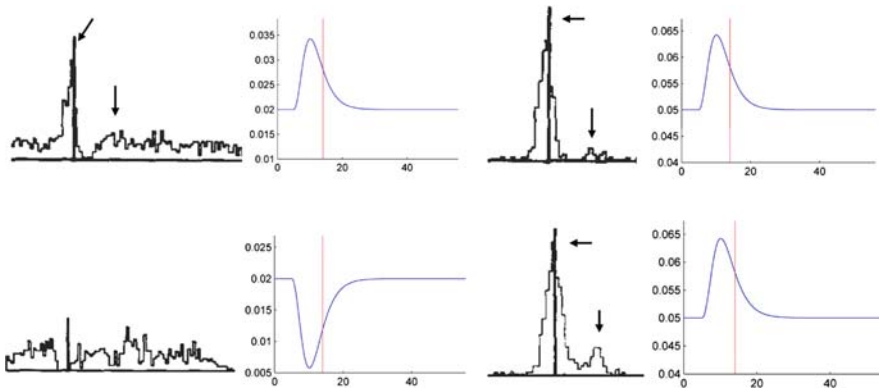


Fig. 10.2: Comparison of peristimulus time histograms (PSTH) of reciprocally organized neurons (column 1; reproduced with permission from [19, Fig. 4A, p. 182], Copyright Springer-Verlag) in area 4, simulated area's 4 reciprocally organized phasic (DVV) cell activities (column 2), PSTH of area's 4 bidirectional neurons (column 3; reproduced with permission from [19, Fig. 4A, p. 182], Copyright Springer-Verlag) and simulated area's 4 co-contractive (P) cells activities (column 4) for a flexion (row 1) and extension (row 2) movements in normal monkey. The vertical bars indicate the onset of movement. Note a clear triphasic AG1-ANT1-AG2 pattern marked with arrows is evident in PSTH of reciprocally and bidirectionally organized neurons. The second AG2 burst is absent in simulated DVV cell activities.

While the reciprocal pattern of muscle activation served to move the joint from an initial to a final position, the antagonist co-contraction served to increase the apparent mechanical stiffness of the joint, thus fixing its posture or stabilizing its course of movement in the presence of external force perturbations. The Renshaw population cell activity was modelled by

$$\frac{dR_i}{dt} = \phi(\lambda B_i - R_i) z_i \max(M_i, 0) - R_i(1.5 + \max(R_j, 0)), \quad (10.5)$$

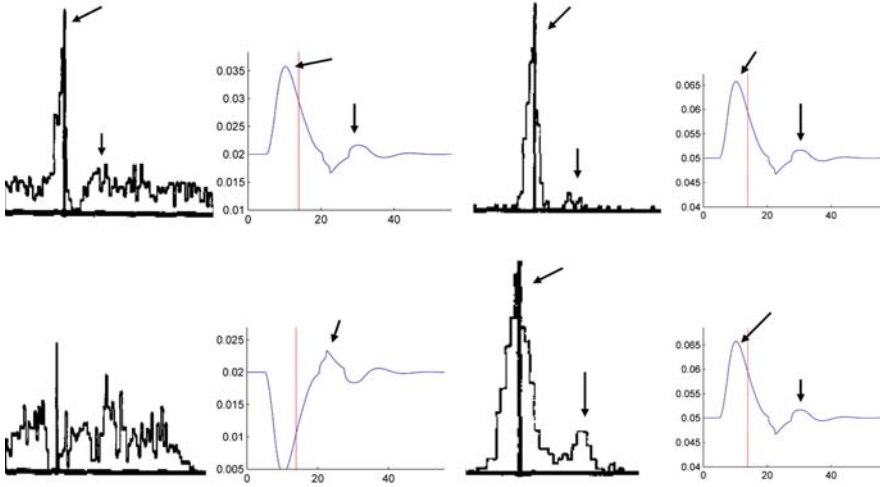


Fig. 10.3: Comparison of peristimulus time histograms (PSTH) of reciprocally organized neurons (column 1; reproduced with permission from [19, Fig. 4A, p. 182], Copyright Springer-Verlag) in area 4, simulated area's 4 reciprocally organized phasic (DVV) cell activities (column 2), PSTH of area's 4 bidirectional neurons (column 3; reproduced with permission from [19, Fig. 4A, p. 182], Copyright Springer-Verlag), and simulated area's 4 co-contractive (P) cells activities (column 4) for a flexion (row 1) and extension (row 2) movements in normal monkey. The vertical bars indicate the onset of movement. Note a clear triphasic AG1-ANT1-AG2 pattern marked with arrows is evident in PSTH of reciprocally and bidirectionally organized neurons. The same triphasic pattern is evident in simulated DVV cell activities. The second peak in simulated activities marked with an arrow arises from the spindle feedback input to area's 5 DV activity.

whereas the α – MN population activity was described by

$$\frac{dM_i}{dt} = \phi(\lambda B_i - M_i) \cdot (A_i + P + \chi \cdot E_i) - (M_i + 2) \cdot (1 + \Omega \cdot \max(R_i, 0)) + \rho \cdot \max(X_i, 0) + \max(I_j^0), \quad (10.6)$$

where X_i was the type I_b interneuron (I_b IN) force feedback, E_i was the stretch feedback, and I_j was the type I_a interneuron. The type I_a interneuron (I_a IN) population activity was defined as

$$\frac{dI_i}{dt} = \phi \cdot (15 - I_i) \cdot (A_i + P + \chi E_i) - I_i(1 + \Omega \cdot \max(R_i, 0) + \max(I_j^0)). \quad (10.7)$$

The I_b IN population activity without dopamine was given by

$$\frac{dX_i}{dt} = \phi \cdot (15 - X_i) F_i - X_i \cdot (0.8 + 2.2 \max(X_j, 0)), \quad (10.8)$$

where F_i was the feedback activity of force-sensitive Golgi tendon organs.

While the extended model was successful in simulating the neuronal activity of the reciprocal and bidirectional cells and proposed for the functional roles in joint movement and stiffness, it failed to simulate the second agonist burst of both the reciprocal and the bidirectional neurons (see columns 1 and 3 of figures 10.2 and 10.3). Due to this failure a biphasic (not triphasic) pattern of α -motorneuronal activation is produced (see Fig. 10.4A). As mentioned earlier, the role of the second agonist burst of the triphasic pattern is to clamp the limb to its final position [29].

To simulate the second observed burst in the reciprocal and bidirectional discharge patterns as well as in the α -MN activities, the extended VITE-FLETE model of Fig. 10.1a [15, 16, 18] was further extended (see Fig. 10.1B) by incorporating the effect of the neuroanatomically observed muscle spindle feedback to the cortex [17]. To model this effect, equation (10.2) was changed to

$$\frac{dV_i}{dt} = 30(-V_i + T_i - A_i + a_w \cdot (W_i(t - \tau) - W_j(t - \tau))), \quad (10.9)$$

where T_i was the target position command, A_i was the current limb position command, a_w was the gain of spindle feedback, and $W_{i,j}$ were the spindle feedback signals from the antagonist muscles. A clear triphasic AG₁-ANT₁-AG₂ reciprocal pattern of cellular activity is evident in figure (column 1 of figure 10.3). Similarly, the activity of bidirectional neurons tuned to both directions of movement is also shown (column 3 of figure 10.3). The simulated marked by an arrow first peak of extension and second peak of flexion reciprocal cells is primarily due to spindle feedback input to DV activity (a feature lacking in [18]). This cortical triphasic pattern of neuronal activation then drives the antagonist α -MNs and produces at their level a similar triphasic pattern of muscle activation (see Fig. 10.4B).

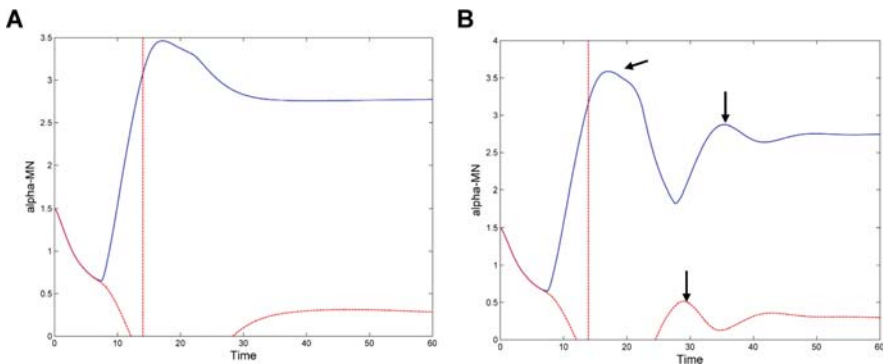


Fig. 10.4: (A) Simulated α -MN activity when the muscle spindle feedback is absent from the cortex. Note a pronounced biphasic AG₁-ANT₁ pattern of muscle activation. The second AG₂ bursts are absent. (B) Simulated α -MN activity when the muscle spindle feedback is present in the cortex. Note a clear triphasic AG₁-ANT₁-AG₂ pattern of muscle activation.

10.4 Conclusion

This chapter has focused on two neural network models of voluntary movement and proprioception under normal conditions. The models seek to explain detailed electromyographic data of rapid single-joint arm movement and identify their neural substrates. The models were successful in providing answers to the questions detailed in the previous sections as well as predicting several characteristics of voluntary movement:

- The reciprocal and bidirectional neurons in primary motor cortex [19] are the two partly independent cortical processes [30] for the reciprocal activation and co-contraction of antagonist muscles in the control of joint rotation and joint stiffness.
- The origin of the triphasic pattern of muscle activation in normal conditions is predicted to be cortical.
- The neural substrates of the triphasic pattern of muscle activation in normal conditions are predicted to be the neuronal discharge patterns of the reciprocal neurons in primary motor cortex.
- The afferent feedback from the muscle spindles to the cortex is responsible for the generation of second agonist burst in the neuronal and EMG activities that clamp the limb to its final position.

Many more predictions regarding voluntary movement control under normal conditions can be found in [18,15,16,17]. In the next chapter, issues regarding *voluntary movement disorganization in Parkinson's disease* will be addressed. In particular, what role, if any, does dopamine depletion in key cortical and spinal cord sites play in the initiation, execution, and control of voluntary movements in Parkinson's disease patients? Does dopamine depletion in basal ganglia, cortex, and spinal cord have any effect on the triphasic pattern of muscle activation? How do the neuronal and EMG variables change when dopamine is depleted?

References

1. Berardelli, A., Dick, J., Rothwell, J., Day, B., Marsden, C. Scaling of the size of the first agonist EMG burst during rapid wrist movements in patients with Parkinson's disease. *J Neurol Neurosurg Psych* **49**, 1273–1279 (1986)
2. Berardelli, A., Hallett, M., Rothwell, J., Agostino, R., Manfredi, M., Thompson, P., Marsden, C. Single-joint rapid arm movement in normal subjects and in patients with motor disorders. *Brain* **119**, 661–674 (1996)
3. Britton, T., Thompson, P., Day, B., Rothwell, J., Findley, L., Marsden, C. Rapid wrist movements in patients with essential tremor. The critical role of the second agonist burst. *Brain* **117**, 39–47 (1994)
4. Brown, S., Cooke, J. Initial agonist burst duration depends on movement amplitude. *Exp Brain Res* **55**, 523–527 (1984)
5. Brown, S., Cooke, J. Movement related phasic muscle activation I. Relations with temporal profile of movement. *J Neurophys* **63**(3), 455–464 (1990)

6. Brown, S., Cooke, J. Movement related phasic muscle activation II. Generation and functional role of the triphasic pattern. *J Neurophysiol* **63**(3), 465–472 (1990)
7. Bullock, D., Grossberg, S. Neural dynamics of planned arm movements: Emergent invariants and speed-accuracy properties during trajectory formation. *Psychol Rev* **95**, 49–90 (1988)
8. Bullock, D., Grossberg, S. VITE and FLETE: Neural modules for trajectory formation and tension control. In: *Volitional Action*. North-Holland, Amsterdam, The Netherlands (1989). 253–297
9. Bullock, D., Grossberg, S. Adaptive neural networks for control of movement trajectories invariant under speed and force rescaling. *Hum Mov Sci* **10**, 3–53 (1991)
10. Bullock, D., Grossberg, S. Emergence of triphasic muscle activation from the nonlinear interactions of central and spinal neural networks circuits. *Hum Mov Sci* **11**, 157–167 (1992)
11. Camarata, P., Parker, R., Park, S., Haines, S., Turner, D., Chae, H., Ebner, T. Effects of MPTP induced hemiparkinsonism on the kinematics of a two-dimensional, multi-joint arm movement in the rhesus monkey. *Neuroscience* **48**(3), 607–619 (1992)
12. Chapman, C.E., Spidalieri, G., Lamarre, Y. Discharge properties of area 5 neurons during arm movements triggered by sensory stimuli in the monkey. *Brain Res* **309**, 63–77 (1984)
13. Contreras-Vidal, J., Grossberg, S., Bullock, D. A neural model of cerebellar learning for arm movement control: Cortico-spino-cerebellar dynamics. *Learn Mem* **3**(6), 475–502 (1997)
14. Corcos, D.M., Jaric, S., Gottlieb, G. Electromyographic analysis of performance enhancement. In: Zelaznik, H.N. (ed.) *Advances in Motor Learning and Control*. Human Kinetics, Vancouver, BC (1996)
15. Cutsuridis, V. Neural model of dopaminergic control of arm movements in Parkinson's disease Bradykinesia. *Artificial Neural Networks, LNCS*, Vol. 4131, pp. 583–591. Springer-Verlag, Berlin (2006)
16. Cutsuridis, V. Biologically inspired neural architectures of voluntary movement in normal and disordered states of the brain. Ph.D. Thesis (2006). Unpublished Ph.D. dissertation. <http://www.cs.stir.ac.uk/vcu/papers/PhD.pdf>
17. Cutsuridis, V. Does reduced spinal reciprocal inhibition lead to co-contraction of antagonist motor units? a modeling study. *Int J Neural Syst* **17**(4), 319–327 (2007)
18. Cutsuridis, V., Perantonis, S. A neural model of Parkinson's disease bradykinesia. *Neural Netw* **19**(4), 354–374 (2006)
19. Doudet, D., Gross, C., Arluison, M., Bioulac, B. Modifications of precentral cortex discharge and EMG activity in monkeys with MPTP induced lesions of DA nigral lesions. *Exp Brain Res* **80**, 177–188 (1990)
20. Feldman, A. Once more on the equilibrium-point hypothesis (λ model) for motor control. *J Mot Behav* **18**, 17–54 (1986)
21. Georgopoulos, A.P., Kalaska, J.F., Caminiti, R., Massey, J.T. On the relations between the direction of two dimensional arm movements and cell discharge in primate motor cortex. *J Neurosci* **2**, 1527–1537 (1982)
22. Ghez, C. Integration in the nervous system, chap. Contributions of Central Programs to Rapid Limb Movement in the Cat, pp. 305–319. Igaku-Shoin, Tokyo (1979)
23. Ghez, C., Gordon, J. Trajectory control in targeted force impulses. I. Role in opposing muscles. *Exp Brain Res* **67**, 225–240 (1987)
24. Ghez, C., Gordon, J. Trajectory control in targeted force impulses. II. Pulse height control. *Exp Brain Res* **67**, 241–252 (1987)
25. Ghez, C., Gordon, J. Trajectory control in targeted force impulses. III. Compensatory adjustments for initial errors. *Exp Brain Res* **67**, 253–269 (1987)
26. Gottlieb, G., Latash, M., Corcos, D., Liubinskas, A., Agarwal, G. Organizing principle for single joint movements: I. agonist-antagonist interactions. *J Neurophys* **13**(6), 1417–1427 (1992)
27. Hallett, C.M., Marsden, G. Ballistic flexion movements of the human thumb. *J Physiol* **294**, 33–50 (1979)
28. Hallett, M., Shahani, B., Young, R. EMG analysis of stereotyped voluntary movements in man. *J Neurol Neurosurg Psychiatr* **38**, 1154–62 (1975)
29. Hannaford, B., Stark, L. Roles of the elements of the triphasic control signal. *Exp Neurol* **90**, 619–634 (1985)

30. Humphrey, D., Reed, D. Separate cortical systems for control of joint movement and joint stiffness: Reciprocal activation and coactivation of antagonist muscles. In: Desmedt, J.E. (ed.) *Motor Control Mechanisms in Health and Disease*, pp. 347–372. Raven Press, New York (1983)
31. Kalaska, J.F., Cohen, D.A.D., Prud'homme, M.J., Hude, M.L. Parietal area 5 neuronal activity encodes movement kinematics, not movement dynamics. *Exp Brain Res* **80**, 351–364 (1990)
32. Schoner, G., Kelso, G. Dynamic pattern generation in behavioural and neural systems. *Science* **239**, 1513–1520 (1988)
33. Stein, R. What muscle variable(s) does the nervous system control in limb movements? *Behav Brain Sci* **5**, 535–577 (1982)
34. Uno, Y., Kawato, M., Suzuki, R. Formation and control of optimum trajectory in human multijoint arm movement-minimumtorque-changemodel. *Biol Cybern* **61**, 89–101 (1989)
35. Wallace, S. An impulse-timing theory for reciprocal control of muscular activity in rapid, discrete movements. *J Mot Behav* **13**, 1144–1160 (1981)
36. Wierzbicka, M., Wiegner, A., Shahani, B. Role of agonist and antagonist muscles in fast arm movements in man. *Exp Brain Res* **63**, 331–340 (1986)